Floquet Theory of Electron Waiting Times in Quantum-Coherent Conductors

David Dasenbrook, Christian Flindt, and Markus Büttiker
Département de Physique Théorique, Université de Genève, 1211 Genève, Switzerland
(Dated: November 12, 2013)

We present a Floquet scattering theory of electron waiting time distributions in periodically driven quantum conductors. We employ a second-quantized formulation that allows us to relate the waiting time distribution to the Floquet scattering matrix of the system. As an application we evaluate the electron waiting time for a periodically driven quantum point contact. A sequence of Lorentzian-shaped voltage pulses generates a train of levitons whose waiting time distribution is investigated. In addition we periodically modulate the transmission of the quantum point contact and find clear fingerprints in the electron waiting times. The distributions of waiting times provide us with a detailed characterization of the dynamical properties of the quantum-coherent conductor.

Introduction.— A surge of interest in dynamic quantum conductors has recently led to a number of groundbreaking experiments [1–5]. An on-demand coherent single-electron source based on a sub-micron capacitor [1, 6] has been experimentally realized and successfully operated in the gigahertz regime [2]. Recently, the fermionic analogue of an optical Hong-Ou-Mandel experiment was performed to demonstrate that two such on-demand sources produce indistinguishable electronic quantum states [3]. Additionally, clean single-particle excitations have been created on top of a Fermi sea by applying a periodic sequence of Lorentzian-shaped voltage pulses to an electrical contact [4, 5] following a pioneering theoretical proposal by Levitov and co-workers [7–9].

These experimental breakthroughs hold promises for future gigahertz quantum electronics with precisely synchronized single-particle operations. One may envision circuit architectures with driven single-electron emitters coupled to the edge states of a quantum Hall conductor (or to the helical edge states in a topological insulator [10, 11]) serving as rail tracks for charge and information carriers by guiding them to beam splitters (quantum point contacts) and particle interferometers for further processing. To facilitate progress towards this goal, a detailed understanding of the single-particle emitters and their statistical properties is required.

In one approach, the full counting statistics of emitted charge is analyzed [12–16]. The charge fluctuations are typically integrated over many periods of the driving and important short-time physics may be lost. In an alternative approach, one considers the distribution of waiting times between charge carriers [17–21]. A quantum theory of electron waiting times has recently been developed for voltage-biased mesoscopic conductors [19], however, so far without an external driving. To describe the statistical properties of coherent single-electron emitters, a theory of waiting time distributions (WTD) for driven mesoscopic conductors is clearly desirable.

In this Letter we develop a quantum formalism for electron waiting times in dynamic mesoscopic conductors described by Floquet scattering theory [22, 23]. Our methodology is applicable to a wide range of periodically driven mesoscopic conductors, for instance the quantum point contact (QPC) depicted in Fig. 1. We illustrate our method by evaluating the WTDs under two different driving schemes. Lorentzian-shaped voltage pulses [7–9] produce clean single-electron excitations (levitons) as recently demonstrated experimentally [4, 5]. We analyze the distribution of waiting times between levitons transmitted through the QPC. We then fix the voltage and investigate the waiting time between electrons with the transmission $T(t)$ of the QPC modulated periodically in time. We focus here on electronic conductors, but our ideas may also be realized in cold atomic gases [24].

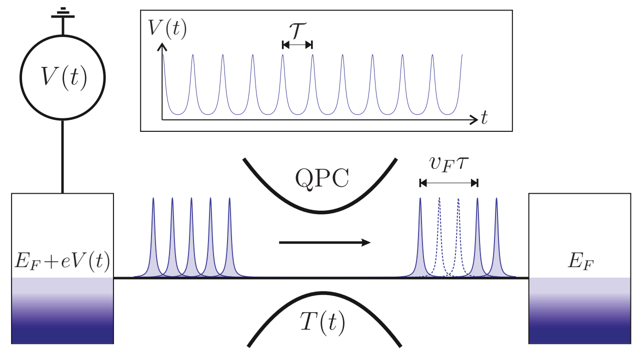

FIG. 1. (color online). Driven quantum point contact. Lorentzian-shaped voltage pulses $V(t)$ with period $\mathcal{T}$ generate a train of clean single-electron excitations (levitons) above the Fermi level E_F. The levitons propagate with the Fermi velocity v_F towards a quantum point contact (QPC) whose transmission $T(t)$ can be controlled. We are interested in the distribution of waiting times τ between transmitted electrons. Reflected (missing) levitons are indicated by dashed lines.

Formalism.— We consider a central scatterer connected to electronic leads. We are interested in the distribution $\mathcal{W}(\tau)$ of waiting times τ between electrons scattered from the left to the right lead, passing a particular point x_0 in the right lead. A fundamental building block of our theory is the idle time probability (ITP) $\Pi(\tau, t_0)$: The ITP is the probability that *no* charges are observed at x_0 in the time interval $[t_0, t_0 + \tau]$. For stationary systems, the ITP is independent of t_0 such that $\Pi(\tau, t_0) = \Pi(\tau)$. The WTD can then be expressed as $\mathcal{W}(\tau) = \langle\tau\rangle\partial_\tau^2\Pi(\tau)$, where $\langle\tau\rangle$ is the mean waiting time [19, 25]. In contrast, for the periodically driven systems of interest here, the ITP is a two-time quantity depending on both t_0 and τ. In that case, the WTD can be evaluated by averaging the ITP over a period of the driving $\mathcal{T}$, using $\Pi(\tau) = \int_0^{\mathcal{T}} \mathrm{d}t_0 \Pi(\tau, t_0)/\mathcal{T}$ above.

Next, we evaluate the ITP for the outgoing many-body state of the scattering problem. The dispersion relation is linear close to the Fermi level, $E_k = \hbar v_F k$, such that all electrons scattered into the right lead propagate with the Fermi velocity v_F towards x_0. The probability of finding no charges at x_0 in the temporal interval $[t_0, t_0 + \tau]$ is then equal to the probability of finding no charges in the spatial interval $[x_0, x_0 + v_F\tau]$ at time $t_0 + \tau$. We thus define the single-particle projection operator $\widehat{Q}_\tau = \int_{x_0}^{x_0+v_F\tau} \mathrm{d}x \,|x\rangle\langle x|$ which measures the probability of finding a given particle in the spatial interval $[x_0, x_0 + v_F\tau]$ [19, 26]. The complementary projector $1 - \widehat{Q}_\tau$ similarly measures the probability of *not* finding the particle. To evaluate the ITP for the outgoing many-body state we proceed with a general second-quantized formulation by introducing the operators $\hat{b}_\alpha^{(\dagger)}(E)$ which annihilate (create) electrons in an outgoing state of lead $\alpha = L, R$ at energy E. We may then write $\widehat{Q}_\tau = \sum_{E,E'} \int_{x_0}^{x_0+v_F\tau} \mathrm{d}x \varphi^*_{R,E'}(x)\varphi_{R,E}(x)\hat{b}^\dagger_R(E)\hat{b}_R(E')$, where $\varphi_{R,E}(x) = \langle x|\,\hat{b}^\dagger_R(E)\,|0\rangle$ and $|0\rangle$ is the vacuum.

The corresponding many-body operator that measures the probability of not finding *any* particles in the spatial interval is the normal-ordered exponential of $-\widehat{Q}_\tau$, see e. g. Refs. [7, 25, 27]. The ITP is then

$$\Pi(\tau, t_0) = \left\langle :e^{-\widehat{Q}_\tau}: \right\rangle_{t_0+\tau}, \tag{1}$$

with $:\ldots:$ denoting normal-ordering of operators and the expectation value is taken with respect to the outgoing many-body state evaluated at the time $t_0 + \tau$. Equation (1) is a powerful formal result. It is also of practical use as it can be applied in a wide range of problems. Below, we consider non-interacting electrons, but Eq. (1) may equally well form the basis of a theory of WTDs in interacting systems. For stationary scattering problems, Eq. (1) reduces to the first-quantized result $\Pi(\tau) = \left\langle \bigotimes_{i=1}^N [1 - \widehat{Q}_\tau] \right\rangle_{t_0+\tau}$ from Ref. [19] with the expectation value taken with respect to a time-evolved Slater determinant describing N particles.

Floquet theory.— We now focus on scatterers that are driven with frequency $\Omega = 2\pi/\mathcal{T}$ and evaluate the ITP using Eq. (1). To this end, Floquet scattering theory provides us with a convenient framework [22, 28]. The scatterer is described by the Floquet scattering matrix $\mathcal{S}$ whose matrix elements $\mathcal{S}_{\alpha\beta}(E_n, E)$ with $E_n = E + n\hbar\Omega$ are the amplitudes for an in-coming electron in lead β with energy E to scatter into lead α having absorbed $(n > 0)$ or emitted $(n < 0)$ $|n|$ energy quanta of size $\hbar\Omega$. The operators for the outgoing states can be expressed in terms of the operators of the incoming states as [22, 28]

$$\hat{b}_\alpha(E) = \sum_\beta \sum_{E_n} \mathcal{S}_{\alpha\beta}(E, E_n)\hat{a}_\beta(E_n). \tag{2}$$

Inserting this relation into Eq. (1), the ITP can be written in terms of the operators $\hat{a}_\beta(E)$ for the incoming states. The evaluation of the ITP then amounts to calculating equilibrium averages of combinations of operators for the incoming states $\hat{a}_\beta(E)$.

At zero temperature, the incoming states are all filled up to the Fermi level. (A voltage difference V between the leads can be included as a time-dependent scattering phase). After some algebra, we then arrive at

$$\Pi(\tau, t_0) = \det(1 - \mathbf{Q}_{\tau,t_0}) \tag{3}$$

where the single-particle matrix elements of $\mathbf{Q}_{\tau,t_0}$ are

$$\begin{aligned}\mathbf{Q}_{\tau,t_0}(E, E') = \sum_{\substack{m=-\lfloor E/\hbar\Omega\rfloor \\ n=-\lfloor E'/\hbar\Omega\rfloor}}^{\infty}\sum^{\infty} &\mathcal{S}^*_{RL}(E_m, E)\mathcal{S}_{RL}(E'_n, E') \\ &\times K_{\tau,t_0}(E_m, E'_n)\Theta(-E)\Theta(-E')\end{aligned} \tag{4}$$

having introduced the kernel $K_{\tau,t_0}(E, E') = 2e^{iqv_F(t_0-\tau/2)} \sin(qv_F\tau/2)/q$ with $q = (E - E')/\hbar v_F$ [19, 26]. In deriving Eq. (4), we concentrated on situations where all particles scattered into the right lead originate from the left lead. We consider the waiting times between particles transmitted through the scatterer above the Fermi level at $E_F = 0$ of the right lead, for example using an appropriate energy filter.

Driven quantum point contact.— We now turn to the setup depicted in Fig. 1, consisting of a QPC connected to source (left) and drain (right) electrodes. We first apply a periodic voltage $V(t)$ to the left electrode and later discuss a time-dependent transmission $T(t)$. The voltage consists of a series of Lorentzian-shaped pulses

$$V(t) = \frac{\hbar}{e} \sum_{n=-\infty}^{\infty} \frac{2\tau_p}{(t - n\mathcal{T})^2 + \tau_p^2} \tag{5}$$

as illustrated in Fig. 1. The width of the pulses is τ_p and the period is $\mathcal{T}$. Remarkably, such pulses lead to clean single-electron excitations without accompanying holes as recently demonstrated experimentally by Dubois *et al.* and hereafter named levitons [4, 5]. The outgoing state can also be created by a mesoscopic capacitor with a slow linear driving protocol [10, 11, 29–32].

We treat the adiabatic regime, where the time scale over which the voltage is modulated is much longer than the time it takes an electron to pass through the scattering region. The Floquet scattering matrix $\mathcal{S}$ can then be related to the "frozen" scattering matrix $\mathcal{S}^f(t)$ at time t as $\mathcal{S}_{\alpha\beta}(E_n, E) = \int_0^{\mathcal{T}} \mathrm{d}t e^{in\Omega t}\mathcal{S}^f_{\alpha\beta}(E, t)/\mathcal{T}$ [22, 28]. The

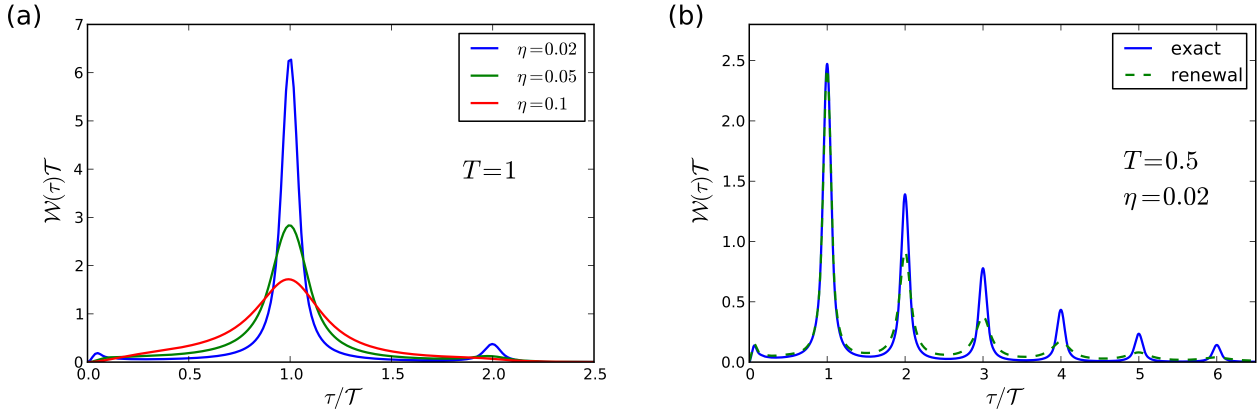

FIG. 2. (color online). Waiting times between levitons. (a) WTDs for levitons with different relative widths η and the QPC fully open ($T = 1$). For small widths, a clear peak in the WTD is observed at the period of the voltage pulses, $\tau = \mathcal{T}$, together with small side peaks. As the pulses start to overlap, the peaks are smeared out. (b) WTD for levitons with the QPC tuned to half transmission ($T = 0.5$). Cycle missing events may now occur as levitons reflect back on the QPC, giving rise to clear peaks at multiples of the period. We compare exact results to the approximation in Eq. (7) based on a renewal assumption.

frozen transmission amplitude is energy-independent and reads $\mathcal{S}^f_{RL}(E,t) = \sqrt{T}\sin[\pi(t/\mathcal{T}+i\eta)]/\sin[\pi(t/\mathcal{T}-i\eta)]$ with $\eta = \tau_p/\mathcal{T}$, see e. g. Ref. [33]. For the Floquet scattering amplitude, we find

$$\mathcal{S}_{RL}(E_n,E) = 2\sqrt{T}\sinh(2\pi\eta)e^{-2\pi\eta n}\Theta(n). \tag{6}$$

For well-separated pulses, $\eta \ll 1$, the scattering amplitude reduces to $\mathcal{S}_{RL}(E_n,E) \simeq 4\pi\sqrt{T}\eta e^{-2\pi\eta n}\Theta(n)$ as in Ref. [33]. For pulses with a large overlap, $\eta \gg 1$, the scattering amplitude $\mathcal{S}_{RL}(E_n,E) \simeq \sqrt{T}\delta_{n,1}$ is that of a QPC with transmission T and static voltage $V_{\rm dc} = \hbar\Omega/e$, see also Eq. (8) below. With the Floquet scattering matrix at hand we proceed by calculating the matrix $\mathbf{Q}_{\tau,t_0}$ in Eq. (4) and the determinant in Eq. (3) to find the WTD.

Figure 2a shows WTDs for different pulse widths with the QPC fully open. The WTDs are all suppressed to zero at $\tau = 0$, independently of the pulse width. This is due to the fermionic statistics which prevents two electrons from being detected at the same time [19]. This suppression would be lifted if we included the spin of the electrons and considered two independent spin channels. With sharp pulses, most levitons are separated by one period of the driving as reflected by the large peak at $\tau = \mathcal{T}$. However, although one excitation is created in each period, the detection of an electron may happen in the (long) tails of the leviton, such that a period is skipped. This gives rise to the small but visible side-peaks at multiples of the period as well as the small peak just after $\tau = 0$. As the pulse width is increased, the peak in the WTD broadens as the waiting time becomes less regular. Finally, for strongly overlapping pulses, the voltage is essentially constant and we recover the results for a dc-biased QPC (not shown) [19].

Figure 2b shows the WTD with the QPC tuned to half transmission. Levitons may now reflect back on the QPC, and cycle-missing events, in which no levitons reach the right electrode within several periods, are very likely. The cycle-missing events give rise to clear peaks at multiples of the period. The effect of the QPC can be understood in a simple picture by resolving the WTD with respect to the number of reflections that have occurred as $\mathcal{W}(\tau) = T\mathcal{W}^{\rm in}_1(\tau) + TR\mathcal{W}^{\rm in}_2(\tau) + TR^2\mathcal{W}^{\rm in}_3(\tau) + \ldots$. The reflection probability is $R = 1-T$ and the $\mathcal{W}^{\rm in}_n(\tau)$'s are the distributions of waiting times between $n+1$ incoming levitons. These are related to the joint probability distributions $\mathcal{W}^{\rm in}_n(\tau_1,\ldots,\tau_n)$ for n successive waiting times between incoming levitons, for example $\mathcal{W}^{\rm in}_2(\tau) = \int_0^\tau {\rm d}t_1 \mathcal{W}^{\rm in}_2(t_1,\tau-t_1)$. Introducing the Laplace transform $\widetilde{\mathcal{W}}(z) = \int_0^\infty {\rm d}\tau \mathcal{W}(\tau)e^{-z\tau}$, we have $\widetilde{\mathcal{W}}^{\rm in}_n(z) = \widetilde{\mathcal{W}}^{\rm in}_n(z,\ldots,z)$. We now make the renewal assumption that successive waiting times are uncorrelated [34] such that the joint WTDs factorize as $\widetilde{\mathcal{W}}^{\rm in}_n(z,\ldots,z) \simeq [\widetilde{\mathcal{W}}^{\rm in}_1(z)]^n$. We can then resum the geometric series $\widetilde{\mathcal{W}}(z) \simeq T\widetilde{\mathcal{W}}^{\rm in}_1(z)\sum_{n=0}^\infty[R\widetilde{\mathcal{W}}^{\rm in}_1(z)]^n$ as

$$\widetilde{\mathcal{W}}(z) \simeq \frac{T\widetilde{\mathcal{W}}^{\rm in}_1(z)}{1-R\widetilde{\mathcal{W}}^{\rm in}_1(z)}. \tag{7}$$

The WTD of the incoming levitons, $\widetilde{\mathcal{W}}^{\rm in}_1(z)$, is the WTD at full transmission ($T = 1$) shown in Fig. 2a.

Equation (7) provides us with a direct test of the renewal assumption of uncorrelated waiting times. Reverting it to the time domain, we can compare Eq. (7) with the exact results in Fig. 2b. The first peak around $\tau = \mathcal{T}$ is governed by the term $T\mathcal{W}^{\rm in}_1(\tau)$, which does not depend on the renewal assumption, and good agreement is found. In contrast, the following peaks are increasingly smeared out under the renewal assumption. This demonstrates that successive waiting times are correlated. The external driving produces a quasi-periodic train of incoming

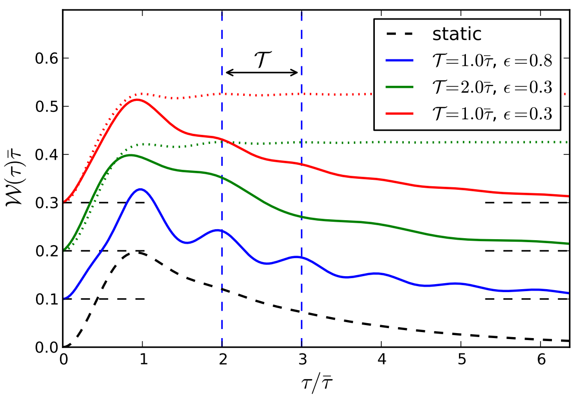

FIG. 3. (color online). Periodically modulated QPC transmission. The WTDs are shifted vertically for clarity. Oscillations with a period of the driving $\mathcal{T}$ are superimposed on the WTD for a static QPC with $T_{\rm av} = 0.4$. The green and red curves are results with a small modulation. The short time expansions, Eq. (9), are shown with dotted lines for comparison. The blue curve shows a WTD with a stronger modulation.

levitons. Thus, a waiting time that is shorter (longer) than the period $\mathcal{T}$ will likely be followed by a waiting time that is longer (shorter) than the period. These correlations, which are responsible for the sharp peaks in Fig. 2b, are omitted under the renewal assumption. We note that the full counting statistics for this problem is always binomial with success probability T and therefore does not distinguish between a static voltage and a series of lorentzian pulses [8]. In contrast, the WTD contains interesting features related to the width of the pulses.

Time-dependent transmission.— We now fix the voltage $V(t) = V$ and instead modulate the transmission probability periodically in time as $T(t) = T_0[1 - \epsilon\sin(\Omega t)]^2$ [35, 36]. The average transmission probability is $T_{\rm av} = T_0(1+\epsilon^2/2)$ and the maximal transmission $T_{\rm max} = T_0(1+\epsilon)^2$ must be smaller than unity. The frozen transmission amplitude from the left to the right lead reads $\mathcal{S}^f_{RL}(E,t) = \sqrt{T(t)}e^{-ieVt/\hbar}$. For the Floquet scattering matrix we find in the adiabatic limit

$$\mathcal{S}_{RL}(E_n, E) = \sqrt{T_0}[\delta_{n,p} + i\epsilon(\delta_{n,p-1} - \delta_{n,p+1})/2], \quad (8)$$

assuming for the sake of simplicity that the applied voltage is a multiple of the modulation quantum, $eV = p\hbar\Omega$, where p is an integer, so that the problem is $\mathcal{T}$-periodic. (The case $qeV = p\hbar\Omega$ with p and q being integers can easily be treated, although the problem becomes $q\mathcal{T}$-periodic). Apart from the central energy band (the Kronecker delta $\delta_{n,p}$) due to the voltage bias, there are two sidebands corresponding to electrons emitting ($\delta_{n,p-1}$) or absorbing ($\delta_{n,p+1}$) a modulation quantum.

Figure 3 shows the WTD for different modulation frequencies. Compared to the static case, the external driving introduces oscillations in the WTD. For weak modulations ($\epsilon \ll 1$) and low transmissions ($T_0 < 1$), the determinant in Eq. (3) can be expanded to lowest order in ϵ and T_0. A detailed calculation then yields

$$\mathcal{W}(\tau) \simeq T_0\left(\frac{g^{(2)}_{\bar{\tau}}(\tau)}{\bar{\tau}} + \epsilon^2\left[\frac{g^{(2)}_{\bar{\tau}_\Omega}(\tau)}{\bar{\tau}_\Omega} + \frac{g^{(2)}_{\bar{\tau}_{-\Omega}}(\tau)}{\bar{\tau}_{-\Omega}}\right]\right), \quad (9)$$

where $g^{(2)}_x(\tau) = 1 - \sin^2(\pi\tau/x)/(\pi\tau/x)^2$ is the two-point correlation function for a static voltage-biased conductor. The expansion is expected to be valid at short times [19] as confirmed by Fig. 3. In Eq. (9), time-scales related to the driving $\bar{\tau}_{\pm\Omega} = h/(eV \pm \hbar\Omega)$ appear in addition to the time-scale associated with the static voltage, $\bar{\tau} = h/eV$. Equation (9) is simply a superposition of correlation functions for a static voltage-biased QPCs with voltages eV and $eV \pm \hbar\Omega$, respectively, reflecting the three energy bands in Eq. (8). Interferences between the bands show up at longer waiting times, leading to the oscillations with period $\mathcal{T}$ in Fig. 3.

Conclusions.— We have developed a Floquet theory of electronic WTDs in periodically driven quantum conductors. We illustrated our method by evaluating the WTDs for a driven QPC, focusing on levitons produced by lorentzian-shaped voltage pulses as well as a periodic modulation of the QPC transmission. For both driving schemes, the WTDs provides us with a detailed characterization of the dynamic quantum conductor, beyond what can be obtained from the full counting statistics alone. Directions for future work include the WTDs for non-adiabatic driving protocols as well as investigations of correlations between electron waiting times.

Acknowledgements.— We thank M. Albert, G. Haack, P. P. Hofer, J. Li, M. Moskalets, and J. R. Ott for helpful discussions. In addition, we thank M. Albert for letting us know about a related work in progress on WTDs of levitons. This work was supported by Swiss NSF and NCCR QSIT.

[1] J. Gabelli, G. Fève, J.-M. Berroir, B. Plaçais, A. Cavanna, B. Etienne, Y. Jin, and D. C. Glattli, Science **313**, 499 (2006).
[2] G. Fève, A. Mahè, J.-M. Berroir, T. Kontos, B. Plaçais, D. C. Glattli, A. Cavanna, B. Etienne, and Y. Jin, Science **316**, 1169 (2007).
[3] E. Bocquillon, V. Freulon, J.-M. Berroir, P. Degiovanni, B. Plaçais, A. Cavanna, Y. Jin, and G. Fève, Science **339**, 1054 (2013).
[4] J. Dubois, T. Jullien, P. Roulleau, F. Portier, P. Roche, A. Cavanna, Y. Jin, W. Wegschneider, and D. C. Glattli, Nature **502**, 659 (2013).
[5] C. Flindt, Nature **502**, 630 (2013).
[6] M. Büttiker, H. Thomas, and A. Prêtre, Phys. Lett. A **180**, 364 (1993).
[7] L. S. Levitov, H. Lee, and G. B. Lesovik, J. Math. Phys. **37**, 4845 (1996).

[8] D. A. Ivanov, H. W. Lee, and L. S. Levitov, Phys. Rev. B **56**, 6839 (1997).
[9] J. Keeling, I. Klich, and L. S. Levitov, Phys. Rev. Lett. **97**, 116403 (2006).
[10] P. P. Hofer and M. Büttiker, arXiv:1307.1225.
[11] A. Inhofer and D. Bercioux, arXiv:1307.1198.
[12] Ya. M. Blanter and M. Büttiker, Phys. Rep. **336**, 1 (2000).
[13] Yu. V. Nazarov, ed., *Quantum Noise in Mesoscopic Physics* (Kluwer, Dordrecht, 2003).
[14] A. Andreev and A. Kamenev, Phys. Rev. Lett. **85**, 1294 (2000).
[15] Yu. Makhlin and A. D. Mirlin, Phys. Rev. Lett. **87**, 276803 (2001).
[16] M. Albert, C. Flindt, and M. Büttiker, Phys. Rev. B **82**, 041407 (2010).
[17] T. Brandes, Ann. Phys. **17**, 477 (2008).
[18] M. Albert, C. Flindt, and M. Büttiker, Phys. Rev. Lett. **107**, 086805 (2011).
[19] M. Albert, G. Haack, C. Flindt, and M. Büttiker, Phys. Rev. Lett. **108**, 186806 (2012).
[20] K. H. Thomas and C. Flindt, Phys. Rev. B **87**, 121405(R) (2013).
[21] L. Rajabi, C. Pöltl, and M. Governale, Phys. Rev. Lett. **111**, 067002 (2013).
[22] M. Moskalets, *Scattering Matrix Approach to Non-Stationary Quantum Transport* (Imperial College Press, 2011).
[23] M. H. Pedersen and M. Büttiker, Phys. Rev. B **58**, 12993 (1998).
[24] J.-P. Brantut, J. Meineke, D. Stadler, S. Krinner, and T. Esslinger, Science **337**, 1069 (2012).
[25] R. Vyas and S. Singh, Phys. Rev. A **38**, 2423 (1988).
[26] F. Hassler, M. V. Suslov, G. M. Graf, M. V. Lebedev, G. B. Lesovik, and G. Blatter, Phys. Rev. B **78**, 165330 (2008).
[27] S. Saito, J. Endo, T. Kodama, A. Tonomura, A. Fukuhara, and K. Ohbayashi, Phys. Lett. A **162**, 442 (1992).
[28] M. Moskalets and M. Büttiker, Phys. Rev. B **66**, 205320 (2002).
[29] J. Keeling, A. V. Shytov, and L. S. Levitov, Phys. Rev. Lett. **101**, 196404 (2008).
[30] F. Battista and P. Samuelsson, Phys. Rev. B **85**, 075428 (2012).
[31] S. Ol'khovskaya, J. Splettstoesser, M. Moskalets, and M. Büttiker, Phys. Rev. Lett. **101**, 166802 (2008).
[32] G. Haack, M. Moskalets, and M. Büttiker, Phys. Rev. B **87**, 201302 (2013).
[33] J. Dubois, T. Jullien, C. Grenier, P. Degiovanni, P. Roulleau, and D. C. Glattli, Phys. Rev. B **88**, 085301 (2013).
[34] D. R. Cox, *Renewal Theory* (Chapman and Hall, London, 1962).
[35] I. Klich and L. S. Levitov, Phys. Rev. Lett. **102**, 100502 (2009).
[36] J. Zhang, Yu. Sherkunov, N. d'Ambrumenil, and B. Muzykantskii, Phys. Rev. B **80**, 245308 (2009).